Journal of Metals, Materials and Minerals, Vol.27 No.1 pp.53-58, 2017

Metallographic Analysis and Electrical Resistivity of the 1045 Steel after being Heat-treated

M. QUIROGA AGURTO, E. MEDRANO ATENCIO, F. A. REYES NAVARRO* and J. G. MIRANDA RAMOS

Laboratorio de Cristales Reales y Aleaciones Metálicas (LABCRAM), Facultad de Ciencias Físicas, Universidad Nacional Mayo de San Marcos (UNMSM), Calle Germán Amézaga 375, Lima, Perú.

Abstract

Herein, it was studied the structural evolution of the AISI 1045 steel water-quenched and oil-quenched, respectively, from a temperature higher than the critical to various temperatures between 800 and 820°C. The two quenching media were used at 16.5°C. Microstructural variations occurred in the quenched 1045 steel. Also, by using the four-terminal sensing, it was measured the evolution of the electrical resistivity of the quenched samples; it was found that quenching at different temperatures provoked a complex behavior. It was noticed a major increase in the electrical resistivity in the case of water-quenched samples. Besides, when compared samples before and after being heat-treated, via a metallographic analysis, it was showed an evolution of the phases of steel, what has a link with the evolution of the electrical resistivity, which was measured according to the increase of the austenitizing temperature.

Keywords: Steel; Electrical resistivity; Quenching; Qustenite; Martensite.

Introduction

Nowadays, steel is one of the alloys of greater commercial interest and use in the world; its heat treatment is a very important *process* as this gives it important mechanical and electrical properties.(1) For example, because electrical resistivity is a fundamental property of materials, its value and dependence on temperature or structural changes become important.(2)

In the scientific literature, namely, there are many experimental and theoretical investigations about the AISI 1045 steel.(3-8) Particularly, it must be cited the research of I. Akhyar and M. Sayuti in 2015.(3) These authors studied, with other values of temperature, a similar research subject, i.e., how heat treatment changes hardness and microstructures of the AISI 1045 steel.

Theoretical Framework

The heat-treated alloy was the AISI 1045 hypoeutectoid steel, which is used in the manufacture of parts of machines, for example, pinions, wedges, shafts, screws, agricultural tools, rivets, etc. The 1045 steel properties can be found in references 7 and 8.(7-8)

Ordinary steel is an alloy of iron, carbon, and other metals (these last in small amounts). However, the potential quality of its hardness is due to carbon, i.e., the degree of hardness is regulated by the carbon content. Likewise, as carbon lowers the melting point of iron, it also provokes in steels an incipient fusion in the grain boundaries. Besides the properties indicated in Table 1, it must be pointed out that iron is a silvery-white metal whose melting temperature is 1,539°C.(9)

In a typical iron-carbon phase diagram, in steel, it can be found the microstructures described in Table 2.(10) In addition to them, bainite is also usually cited; however, it is more important in alloy steels

Experimental Methods

Concerning quenching, in this process, the samples were heated in a furnace built in laboratory

* Corresponding author: E-mail: felipe.reyes@unmsm.edu.pe

DOI: 10.14456/jmmm.2017.8

LABCRAM in UNMSM.[11] Basically, it is a vertical tube furnace with internal diameter of approximately 3.5 cm, and a depth of approximately 14.5 cm; besides, it has a power of 750 W and a maximum heating rate of 13.95 ±1°C/min (temperature was monitored by an immersion probe k-type thermocouple).

Table 1. Properties and types of Iron and Steels.

Allotropic forms of Iron		
Iron α	Iron γ	Iron δ
It occurs < 910°C.	It occurs 910-1,401°C.	It occurs 1,401-1,539°C.
Lattice BCC.	Lattice FCC.	Lattice BCC.
a=0.2860 nm.		
<768°C ferromagnetic.		
>768°C paramagnetic.		
Combinations of Iron and Carbon		
Iron α	Steel	Casting
<0.008% C	0.008-2.11% C	>2.11% C. It cannot be hardened.
Steels		
Known since approximately 3,000 BC. Historically, steel industry begun in the 1,850s, when the Bessemer process was discovered.		
Carbon steels		
Mild steels (low carbon)	Semi-hard steels (medium carbon)	Hard steels (high carbon)
0.07-0.30% C	0.30-0.60 % C	0.60-1.4% C

Table 2. Microstructures present in an iron-carbon phase diagram.

Ferrite	Austenite	Cementite	Pearlite	Martensite
Solid solution. It contains until 0.008% C at 21.11°C. Lattice BCC. Known as Iron α.	It accepts up to 2.0% C. Unstable < 386.11°C (in other alloys, it is stable at room temperature). Ductility, hardening by deformation. Lattice FCC. Non-magnetic Known as Iron γ.	It may contain 6.67-6.69% C. The hardest and most brittle microstructure. Its hardness reach 960 Vickers. Orthorhombic parallelepiped. Magnetic until 210°C. Called iron carbide	Eutectoid mixture originated from the decomposition of austenite at 723°C. It results of the simultaneous precipitation of ferrite and cementite particles. It usually has 0.80% C and causes steel to be more ductile.	It appears in the quenched carbon steel when the cooling rate from the austenite is fast enough [10]. A very hard microstructure. It occurs in a sudden shearing process without diffusion

Microscopic Analysis

To observe and study the microstructures of the samples, with a 400X magnification, it was used an optical metallographic microscope, Euromex Mic. 1060/62. Previously, the surface of each sample had been deburred and, subsequently, polished. Next, the samples were chemically attacked with the 2% Nital reagent for different times of exposure, which had a special role because the evolution of the microstructure was different for each sample.

Microanalysis allows to determine, e.g., size and shape of the grains, arrangement of the phases, components of the alloy, as well as reveal characteristic structures after some types of treatments.[12,13] The chemical attack with Nital revealed only one type of microstructure of steel (ferrite). All steel with less than 0.85% C, when passing through an annealing process forms two types of phases, one called pearlite and the other, ferrite. The latter has 0.008% C and is not affected by the reagent; meanwhile, the former has 0.85% C and its surface is destroyed when exposed to Nital.

Thus, the ferrite surface was flat and the light reflected onto it returned to the chamber so that it appeared as a light region in micrographs; meanwhile, the pearlite crystal had an irregular surface scattering the light so that it appeared as a dark region. In addition, in the ferrite grain boundary, *descaling* by Nital occurred; therefore, the edges of the crystals appeared dark in the micrographs.

The four-terminal sensing

This standard procedure allowed us to measure the electrical resistivity.[14-15] As the thickness of the samples was not very small compared to the separation of the terminals, it was considered both the terminals were infinitesimals and the lateral dimensions of the samples were semi-infinite. In our experimental arrangement, the potential difference of the central terminals was measured with a Keithley 2,182 high accuracy nanovoltmeter, with an accuracy of ± 0.1%.

For calibration at room temperature, voltage and electrical current were measured for 6 non-heat-treated samples from the acquired 1045 steel; the obtained values of ρ were compared with those registered in the literature.[16] Figure 1 shows the values obtained from the electrical resistivity at room temperature for the 6 aforementioned samples. When compared the obtained values with the reference values in the ASTM[16], it was found a percent error of ±0.12%.

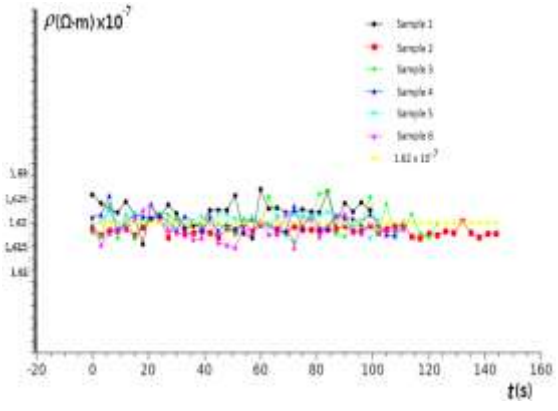

Figure 1. The electric resistivity of the non-heat-treated 1045 steel at 16.5°C.

Results and Discussion

For 11 samples of the 1045 steel, experimental results were obtained; one had no heat treatment, and the other ten were quenched at 800, 805, 810, 815 and 820°C. Namely, five out of these ten samples were cooled in water and the other five samples, in mineral oil.

Concerning the non-heat-treated sample, a micrograph is shown in Figure 2. Therein, it is noticed phases ferrite and pearlite, which correspond to annealed steel. The pearlite crystals look dark because they were descaled when exposed to Nital; on the contrary, the ferrite crystals look light due to their low carbon concentration and, therefore, little reaction to Nital.

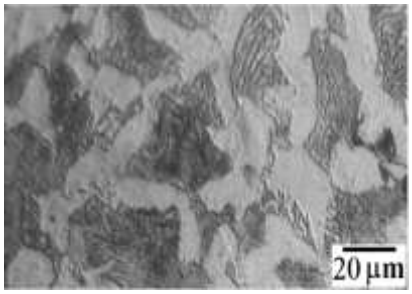

Figure 2., Micrograph of the non-heat-treated 1045 steel at 16.5°C. The scale bar is indicated

Results from microscopy after water quenching

Figure.3a shows micrographs of the water-quenched samples. Because the microstructure of the 1045 steel changed as the temperature increased, it was possible to observe and compare how the water-quenched samples were changing their structure; it was noticed the presence of the martensite phase, which is typical of the quenched steels. Thus, it was observed acicular shapes with relief effects produced by shear mechanisms, what is a proof that the martensite formation resulted from almost instantaneous transformations (without diffusion) in certain crystallographic planes of the austenite lattice.

As a consequence of the quenching at 800°C, the martensite phase appeared; the martensite crystals were larger when the austenite grains were larger, too. The crystal lattice of martensite is normally oriented with respect to the crystal lattice of austenite (the initial crystals are oriented each other at 60 or 120 °C [9]). In samples quenched at 805, 810 and 815°C, the presence of the martensite phase was also noticed. In the sample quenched at 820°C, in addition to martensite, it was observed how the grain boundaries suggested an increase in the *grain size* when compared to that from samples quenched at the other temperatures.

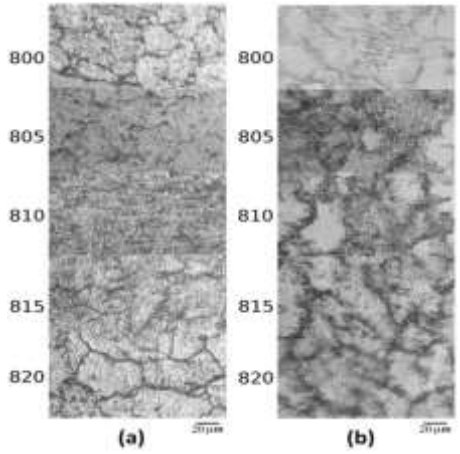

Figure 3. For the 1045 steel, (a) micrographs of water-quenched samples; (b) micrographs of oil-quenched samples. The austenitizing temperatures and the scale bars are indicated.

Results from microscopy after oil quenching

Figure 3b shows micrographs of oil- quenched samples. The one quenched at 800°C showed an incipient structure of martensite. In the sample quenched at 805°C, a major development of martensite was observed. Likewise, in the samples quenched at 810, 815 and 820°C, it was also noticed the presence of the martensite phase albeit to a lesser extent than the previous cases; the grain boundaries also indicated an increase in the grain size regarding that from samples quenched at the other temperature

Results from electrical resistivity

Table 3 shows the values of electrical resistivity obtained from the four-terminal sensing for different T_{Aus}. In this table, it was noticed the variation of the electrical resistivity with respect to the initial one. Because of the subsequent rapid cooling of the material, which had an austenitic structure, it was originated the martensitic transformation where the material's crystal structure had been transformed from FCC to BCT.[17] As a consequence of this transformation, in the final microstructure, dislocations, voids, internal tensions and fine discontinuities arose. What increased the electrical resistivity of the material, i.e., the presence of martensite was accompanied by an increase in the electrical resistivity. Figure. 1 has already shown the electrical resistivity for the acquired steel sample.

Table 3. Austenitizing temperatures and electric resistivity after quenching in water and oil, respectively.

T_{Aus} (°C)	ρ (Ω·m) × 10^{-7}	
	Water quenching	Oil quenching
800	2.416 ± 0.00327	1.780 ± 0.00391
805	2.181 ± 0.00596	2.025 ± 0.00438
810	2.164 ± 0.00416	1.642 ± 0.00268
815	2.174 ± 0.00263	1.703 ± 0.00270
820	2.513 ± 0.00342	1.763 ± 0.00253

For the samples quenched in water and in oil, respectively, it was noticed an increase in the electrical resistivity (from 2.165×10^{-7} to 2.513×10^{-7} Ω·m for water-quenched samples and from 1.642×10^{-7} to 2.026×10^{-7} Ω·m for oil-quenched samples

Results according to austenitizing temperatures

Figure 4 shows how the electrical resistivity evolved as it was increased the austenitizing temperature chosen for the quenching in water and oil, respectively. In this graph, it was clearly noticed that, for water-quenched samples, the evolution of the electrical resistivity was very different to the one for oil-quenched samples; it was noticed a major increase in this property in the case of water quenching. Next, below it is analyzed Figure.4 along with Figure. 3(a) and Figure.3(b), respectively.

On the one hand, there were water-quenched samples. Thus, for the one quenched at 800°C, the electrical resistivity increased from 1.62×10^{-7} to 2.416×10^{-7} Ω·m (non-heat-treated and quenched in water, respectively). Besides, according to micrographs of Figure 3(a), the presence of themartensite phase was observed; this phase provoked an increase in the electrical resistivity because the material's crystal structure had been transformed from an FCC to a BCT lattice.

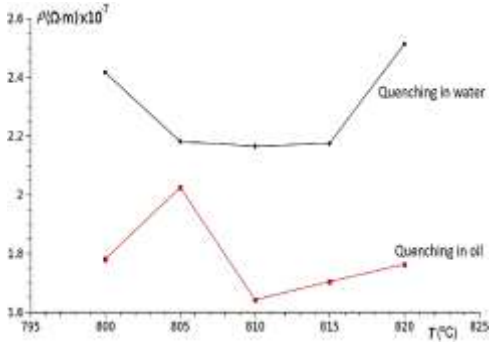

Figure 4. Electric resistivity versus austenitizing temperature. It shows results for quenching in water and oil,too.

For the sample quenched at 805°C, it was obtained a value of 2.181×10^{-7} Ω·m, which was higher than the one of the non-heat-treated sample but less than the one of the sample quenched at 800°C. This was explained as follows: As the formed martensite phase depended on the evolution of the grains forming from the austenite phase, the austenite FCC lattice expanded to give way to the carbon atoms up to a certain point, wherein decreased the development of the grains of austenite; thus the evolution of the grain reduced, after cooling (see Figure. 3(a) for quenching at 805°C). Consequently, the electrical resistivity lowered

For T_{Aus}= 810°C, the obtained electrical resistivity was 2.164×10^{-7} Ω·m. Figure.3a shows that the development of the grain had not varied much due to the slow growth of the austenite phase; what is important to this development after the corresponding coolin

For T_{Aus}= 815°C, it was observed a slight increase in the electrical resistivity up to 2.174×10^{-7} Ω·m; this was due to the slow growth of the austenite phase, what gave way to both a greater development of grains after-cooling and martensite formation at quenching temperature. Besides, in analyzing Figure. 3a for 815°C, it was noticed that the development was greater than in the case of 810°C, what explained why the electrical resistivity increased.

At T_{Aus}= 820°C, it was obtained 2.513×10^{-7} Ω·m, which was the greater value because both the martensite had been formed in a greater proportion and the grains were more evolved (see Figure. 3(a).

On the other hand, there were samples oil-quenched. Thus, from the same Figure. 4, for the sample quenched in oil at 800°C, it was noticed an increase of the electrical resistivity up to 1.78×10^{-7} Ω·m. This increase was due to the presence of the martensite phase; however, in the micrograph of Figure. 3b, the presence of the ferrite phase was still noticed. This was because unlike water cooling, one of the properties of oil cooling is the formation of a jacket steam, which is called layered boiling. This caused the cooling rate to be relatively slow, decreasing the temperature below Ac_3; thus, the austenite phase formed before the martensite phase did (it happened in a fraction of a second). As a result, at the end, there was the presence of martensite and ferrite; consequently, the electrical resistivity increased. Likewise, as in this process, the internal stresses were reduced in comparison with the water quenching, the electrical resistivity did not exceed the one of the water-quenched sample.

For the sample quenched at 805°C, it was observed the presences of ferrite and incipient martensite inside grains looking like ferrite. In Figure 3b, micrograph shows a major presence of this phase, consequently, the electrical resistivity reached a value of 2.025×10^{-7} Ω·m.

For the sample quenched at 810°C, it was still observed the presence of ferrite, which seemed to be stabilized because, from this value of temperature, a sustained growth of the electrical resistivity was maintained. Thus, for quenching at 810°C, it was obtained 1.642×10^{-7} Ω·m; and for 815 and 820°C, 1.703×10^{-7} Ω·m and 1.763×10^{-7} Ω·m, respectively. As shown in the respective micrograph in Figure. 3b, at these temperatures the presence of the martensite phase extended throughout sample and it was evolving more and more. Thus, the greater the presence of martensite was, the higher the electrical resistivity was.

Finally, as the chosen austenitizing temperatures were close to Ac_3 (where the temperature was likely to fall at an instant), it was noticed a complex behavior of the electrical resistivity; however, far from Ac_3, the electrical resistivity grew in a sustained way.

Conclusions

Microstructural variations occurred in the quenched 1045 steel have been observed. As the austenitizing temperature increased, and after a rapid cooling, significant variations occurred in both the morphology of the martensite (due to the induction of non-diffusive processes) and the electrical resistivity. Thus, the dependence of the electrical resistivity on the heat treatment was evidenced. Besides, for the water-quenched samples, there was a relation between the electrical

resistivity and the evolution of the grains formed from the austenite phase, i.e., the evolution of the martensite grains, which caused the electrical resistivity to vary.

Furthermore, when compared the obtained values of the electrical resistivity for the samples quenched, respectively, in water and oil, the former were higher than the latter. What can be explained by the fact that unlike water quenching, oil quenching reduced the internal stresses produced during the sudden formation of the martensite phase. Finally, for the oil-quenched samples, the presence of the ferrite phase was also observed.

Acknowledgments

Special thanks to Prof. L. Malpartida for his comments to improve this work

References

1. Akron Steel Treating Company. (1987). Modern Steels and their properties: Carbon and Alloy-Steel Bars and Rods.

2. S. Klein, L. Mujica Roncery, M. Walter, S. Weber, and W. Theisen. (2017). Diffusion processes during cementite precipitation and their impact on electrical and thermal conductivity of a heat-treatable steel, *J. Mater. Sci.* **52**: 375-390.

3. I. Akhyar and M. Sayuti. (2015). Effect of heat treatment on hardness and microstructures of AISI 1045, Advanced Materials Research. 119: 575-579.

4. K. Gao, X. Qin, Z. Wang, H. Chen, S. Zhu, Y. Liu and Y. Song. (2014). Numerical and experimental analysis of 3D spot induction hardening of AISI 1045 steel. *J. Mater. Process. Technol.* **214,** Iss. 11: 2425-2433.

5. S. Taghizadeh, A. Safarian, Sh. Jalali and A. Salimiasl. (2013). Developing a model for hardness prediction in water-quenched and quenched AISI 1045 steel through an artificial neural lattice. *Materials & Design*. **51**: 530-535.

6. A. Kumar Sinha. (2007). Steel namenclature, In Chap. 1 of *Steel Heat Treatment Handbook*, edited by George E. Totten, CRC press (Taylor & Francis Group).

7. J. R. Davis (Editor). (1998). *Metals Handbook* Desk Edition, Second Edition, pp. 153–173, ASM International.

8. G. E. Totten (Editor). 2007. *Steel Heat Treatment: Equipment and Process Design*, CRC press (Taylor & Francis Group).

9. Y. M. Lajtin. (1973). *Metalografía y tratamiento térmico de los metales* (*Metallography and Heat Treatment of Metals*), Editorial Mir.

10. A. V. Sverdlin and A. R. Ness. (2007). Fundamental concepts in Steel heat treatment, *IN Chap. 3 of Steel Heat Teatment Handbook*, edited by George E. Totten. CRC press (Taylor & Francis Group).

11. M. Quiroga Agurto. (2009). Estudio y medida de la resistividad eléctrica del acero 1045 después de un tratamiento térmico (Study and measurement of the electrical resistivity of the 1045 steel after a heat treatment), *Licentiate thesis, UNMSM*.

12. Dr. E. J. Dubox. (1974). Prácticas de Metalografia (Metallographic Practices), *Ediciones Marymar*, Argentina

1 3
1 . 4

15. A. P. Schuetze, W. Lewis, Ch. Brown and W.J. Geerts (2004). A laboratory on the four-point probe technique. *Am. J. Phys.* 72(2): 149-153.

16. ASTM International. (1998). Standard Test Method for D-C Resistance or Conductance of Moderately Conductive Materials. D4496-87.

17. S. K. Akav, M. Yazici and A. Avinc. (2009). The effect of heat treatments on physical properties of a low carbon steel, *Preceedings of the Romanian Academy, Series A*, 10(1): 000-000(sic).